International Journal of Greenhouse Gas Control 83 (2019) 265–281

Contents lists available at ScienceDirect

International Journal of Greenhouse Gas Control

journal homepage: www.elsevier.com/locate/ijggc

The potential of chemical looping combustion using the gas switching concept to eliminate the energy penalty of CO_2 capture

Carlos Arnaiz del Pozo[b], Schalk Cloete[a], Jan Hendrik Cloete[c], Ángel Jiménez Álvaro[b], Shahriar Amini[a,*]

[a] SINTEF Industry, Trondheim, Norway
[b] Universidad Politécnica de Madrid, Madrid, Spain
[c] Norwegian University of Science and Technology, Trondheim, Norway

ARTICLE INFO

Keywords:
Gas switching combustion
CO_2 capture
Energy penalty
Efficiency
Integrated gasification combined cycle

ABSTRACT

Energy penalty is the primary challenge facing CO_2 capture and storage (CCS) technology. One possible solution to this challenge is gas switching combustion (GSC): a promising technology for gaseous fuel combustion with integrated CO_2 capture at almost no direct energy penalty. However, previous work showed that GSC integrated into an IGCC power plant still imposed an energy penalty of 5.7%-points relative to an unabated IGCC plant. This penalty originates mainly from the maximum temperature limitation of the GSC reactors and inefficient power production from the CO_2-rich stream. Addressing these challenges via an additional combustor after the GSC reactors and improved heat integration successfully eliminated the aforementioned energy penalty, although feeding carbon-containing fuels to the additional combustor reduces the CO_2 capture ratio. Furthermore, GSC presents two channels for exceeding the efficiency of an unabated benchmark plant: 1) the high steam partial pressure in the CO_2-rich stream allows most of the steam condensation enthalpy to be recovered and 2) pre-combustion gas clean-up can potentially be replaced with post-combustion clean-up because pollutants remain concentrated in the CO_2-rich stream. In combination, these effects can boost plant efficiency by a further 2%-points, exceeding the efficiency of an unabated IGCC plant. Ultimately, the most efficient plant evaluated in this study achieved 50.9% efficiency with 80.7% CO_2 capture. The GSC-IGCC power plant can therefore solve the most fundamental challenge facing CCS and more detailed feasibility studies are strongly recommended.

1. Introduction

Climate change resulting from anthropogenic greenhouse gas emissions is a key challenge in the likely future scenario of rising energy demand due to continued global growth in population and prosperity. Given the continued global reliance on fossil fuels for 86% of primary energy consumption (BP, 2018), the Paris Climate Accord (UNFCCC, 2015) objective of limiting global temperature rise to "well below 2 °C" appears increasingly unlikely.

Many pathways are available for reducing greenhouse gas emissions. Among these, CO_2 capture and storage (CCS) is arguably the most important when deep emissions reductions are targeted. The Fifth IPCC report (IPCC, 2014) found that most models could not achieve an emissions target consistent with the Paris Climate Accord if CCS was not included as an option. The few models that achieved the required emissions reductions showed a median 140% increase in cost relative to the case where all technologies are included.

Unfortunately, CCS technology deployment is currently lagging far behind the trajectory required for capping global temperature rise below 2 °C (IEA, 2018). This slow expansion rate is related to the prohibitive cost of first generation CCS technologies, which require CO_2 prices in excess of $60/ton to achieve competitiveness in the largest single global emissions source: coal fired power plants (Rubin et al., 2015). It is highly unlikely that such CO_2 prices will emerge on a sufficiently large scale within the timeframes required by climate science.

The energy penalty of CO_2 capture is the primary cost driver of CCS, typically increasing the fuel consumption per unit electricity by 30% in coal fired power plants (Rubin et al., 2015). This energy penalty not only increases the fuel cost, but also the specific capital cost ($/kW) since a larger plant is required to produce a given power output. Furthermore, the increase in fuel consumption substantially increases the environmental impact of CCS technologies due to CO_2 emissions and other environmental impacts related to additional fuel production and combustion (Marx et al., 2011). Furthermore, the energy penalty

* Corresponding author at: S.P. Andersens vei 15B, 7031, Trondheim, Norway.
E-mail address: shahriar.amini@sintef.no (S. Amini).

https://doi.org/10.1016/j.ijggc.2019.01.018
Received 30 July 2018; Received in revised form 21 December 2018; Accepted 23 January 2019
Available online 08 March 2019

Nomenclature

Main symbols

C_p	Heat capacity (J/kmol/K)
F	Molar flow rate (kmol/s)
ΔH_k^R	Reference enthalpy of reaction (J/kmol)
h	Enthalpy (J/mol)
N	Amount of species (kmol)
P	Pressure (Pa)
R	Reaction rate (kmol/s)
R_0	Universal gas constant (J/kmol.K)
s	Stoichiometric coefficient
T	Temperature (K)
V	Volume (m^3)
ρ	Density (kg/m^3)
y	Mole fraction

Subscripts and superscripts

g	Gas
i, j	Species index
k	Reaction index
s	Solids

Acronyms

ASU	Air separation unit
CCS	CO2 capture and storage
CLC	Chemical looping combustion
CPU	CO2 purification unit
CGCU	Cold gas clean-up
HHV	Higher heating value
GSC	Gas switching combustion
GSOP	Gas switching oxygen production
HRSG	Heat recovery steam generator
HGCU	Hot gas clean-up
IGCC	Integrated gasification combined cycle
LHV	Lower heating value
LH	Lock hoppers
NG	Natural gas
SEC	Syngas effluent cooler
TIT	Turbine inlet temperature
TOT	Turbine outlet temperature
WFGD	Wet flue gas desulphurization

reduces the actual CO_2 avoidance of CCS significantly below the fraction of produced CO_2 that is successfully captured, while also increasing the quantity of CO_2 that must be safely transported and stored.

For all these reasons, energy penalty reductions have long been the primary focus of CO_2 capture research and development. Among current approaches, chemical looping combustion (CLC) is the most fundamentally promising because it can inherently achieve CO_2 capture with almost no direct energy penalty (Ishida et al., 1987; Lyngfelt et al., 2001). CLC makes use of an oxygen carrier to carry out combustion of the fuel in a nitrogen free environment, instead of a typical combustion chamber. An oxygen carrier material, typically a metal oxide, is oxidized by air in one reactor and subsequently transported to another reactor where it is reduced by a fuel gas. In this way, the two CLC reactors yield separate streams of hot depleted air for driving a power cycle and combustion products that require only steam condensation to achieve a high purity CO_2 stream.

Despite the ability of CLC to alleviate the primary CCS bottleneck of energy penalty, development of this technology has been relatively slow. A prominent reason for the relatively slow scale-up of CLC is the challenge of operating a system of two interconnected fluidized bed reactors with large quantities of solids transfer between them. The solids circulation rate must be tightly controlled to maintain mass and energy balances, but solids circulation is strongly dependent on the prevailing hydrodynamics in both reactors. CLC scale-up must therefore be done incrementally to ensure that the hydrodynamic behaviour required for reliable solids circulation is preserved. The sensitivity of solids circulation rate to reactor hydrodynamics also makes the CLC concept inherently inflexible regarding gas feed rate.

These challenges are magnified further when operating under pressurized conditions to allow for efficient power production with gaseous fuels using a combined cycle. As illustrated in a recent review by Mattisson et al. (2018), the scale-up of gas-fuelled CLC experimental

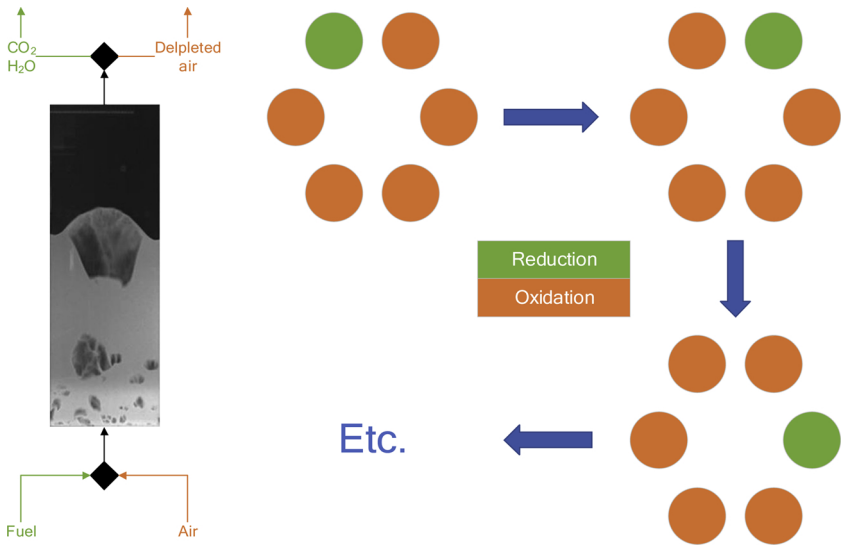

Fig. 1. Left: The gas switching combustion principle. Right: A cluster of gas switching combustion reactors operating as a steady state processing unit.

demonstrations has been limited over the reviewed publications spanning a 14-year period. In addition, only one of the reviewed studies was completed under pressurized conditions (Wang et al., 2010) where the highest pressure investigated (5 bar) is still well below the requirements for an efficient combined cycle (~20 bar).

In-situ gasification CLC is one technology that can avoid the need for pressurized operation and this variant of CLC has shown more promising rates of scale-up according to the studies reviewed by Mattisson et al. (2018). In this case, the requirement to directly feed solid fuel to the reduction reactor introduces several additional challenges such as fuel slip from syngas produced near the top of the reactor bed, the need for a carbon stripper unit to prevent char from leaking to the oxidation reactor, and the demand for a very cheap oxygen carrier that can have a short active lifetime due to ash exposure or losses with ash removal (Abad et al., 2015; Lyngfelt, 2014). However, progress towards commercialization can be accelerated by drawing from similarities with circulating fluidized bed boilers in operation today (Lyngfelt and Leckner, 2015).

These challenges can be avoided by completing the gasification of solid fuels outside the CLC reactors, but such configurations must operate under pressurized conditions to achieve competitive efficiencies. Several reactor concepts have been proposed to simplify the pressurized operation required in such gaseous fuel CLC applications including packed bed CLC (Hamers et al., 2013; Noorman et al., 2007), gas switching combustion (Zaabout et al., 2015, 2013) and rotating reactors (Hakonsen and Blom, 2011). This work will focus on gas switching combustion (GSC) based on its simplicity relative to conventional CLC and rotating reactors as well as its avoidance of the material-related challenges facing packed bed CLC (Cloete et al., 2016).

GSC utilizes standalone bubbling fluidized bed reactors containing an oxygen carrier material that is alternatively exposed to fuel and air streams (Fig. 1, left). In this way, the need for solids circulation is completely avoided, with the cyclones and loop seals of CLC being replaced by simple inlet and outlet valves in GSC. Furthermore, standalone bubbling fluidized bed reactors are simple to pressurize and operate under flexible gas throughput rates. As illustrated in Fig. 1 (right), the transient operation of individual GSC reactors requires a cluster of several reactors to create a steady-state processing unit.

Autothermal pressurized GSC operation has been successfully demonstrated with scalable oxygen carrier materials (Zaabout et al., 2017; Zaabout et al., 2019). Given the simplicity of scaling up a standalone bubbling fluidized bed reactor, these demonstration studies can prompt rapid scale-up and commercialization of the GSC technology if the business case is strong enough.

As with all CCS technologies, the energy penalty is a vital part of the business case. Power plant simulation studies of GSC integrated into an IGCC power plant have been carried out (Cloete et al., 2015, 2017), finding an efficiency of 41.6% with 90% CO_2 avoidance. Even though the achieved efficiency clearly outperforms first generation pre-combustion CO_2 capture at 38% efficiency, a significant energy penalty is still incurred relative to an unabated (no CO_2 capture) IGCC plant with an advanced gas turbine (TIT = 1360 °C) at 47.3% efficiency (Cloete et al., 2015).

The GSC-IGCC configuration investigated in the aforementioned works is therefore promising, but certainly not revolutionary. Substantial further efficiency gains will be required to realize the gamechanging potential of GSC technology. This study will evaluate several pathways through which such gains can be achieved, allowing GSC to match or even exceed the efficiency of an unabated IGCC power plant.

2. Pathways towards maximum efficiency

Reactor pressure drop is the only direct energy penalty imposed by GSC. This penalty is only about 0.25%-points for the present study, but GSC faces two more important challenges that cause larger reductions in its electric efficiency. Both these challenges can be overcome, potentially allowing GSC to achieve similar efficiencies to an unabated IGCC power plant.

In addition, GSC presents two interesting opportunities for additional efficiency gains that are not accessible to a conventional plant. These benefits open the potential for GSC to exceed the efficiency of an unabated IGCC benchmark.

The two challenges and opportunities will be discussed in more detail below.

2.1. Challenge 1: limited reactor temperature

The most important efficiency-related challenge faced by the GSC concept is that the maximum achievable reactor temperature will be limited by the oxygen carrier, reactor body, outlet valves and filters. To date, studies have assumed the maximum achievable reactor temperature to be 1200 °C, generally allowing for an average turbine inlet temperature (TIT) of about 1150 °C. This is well below the temperatures achievable by modern gas turbines, resulting in an estimated 4%-point loss relative to the unabated IGCC benchmark with 1360 °C TIT assessed in the first GSC-IGCC power plant simulation (Cloete et al., 2015).

This challenge can be overcome by combusting a relatively small additional quantity of gaseous fuel after the GSC reactors to increase the temperature to the maximum achievable TIT. The simplest option is to simply use a carbon-containing fuel, either syngas from the gasifier or natural gas (NG). Naturally, this will reduce the CO_2 capture efficiency of the plant. This strategy has been briefly investigated by Zerobin and Pröll (2017) where it was found that using only 10% of the fuel in a combustor after the CLC reactors caused a 3%-point increase in efficiency.

High CO_2 capture rates can be maintained by doing the additional firing with hydrogen instead. Producing hydrogen from hydrocarbon fuels with CO_2 capture imposes a significant efficiency penalty, but highly efficient methods based on the chemical looping principle, such as steam-iron water splitting (Rydén and Arjmand, 2012), membrane-assisted chemical looping reforming (Spallina et al., 2016) and gas switching reforming (Wassie et al., 2017), are currently emerging. Efficient integration of such technologies into the power plant for additional firing with H_2 can retain most of the efficiency gain from higher TIT.

One possible technology development pathway is to build a GSC-IGCC power plant with additional firing using readily available hydrocarbon fuels under the knowledge that retrofitting for H_2 firing can be done relatively easily at a later stage if CO_2 prices become high enough. As shown later in this study, such a partial CO_2 capture plant can still achieve above 80% CO_2 capture with no energy penalty.

This partial capture GSC-IGCC plant will also be well suited to load following operation in a future energy system with high CO_2 prices. Full load operation at maximum TIT will only occur when the wholesale electricity price is high enough to ensure profitability despite CO_2 emissions costs. When the wholesale price becomes lower during times of lower electricity demand, the plant can respond appropriately by entering part-load operation, which requires a lower TIT. In this case, additional firing is not required, allowing the plant to achieve maximum CO_2 capture and minimum CO_2 emissions costs.

2.2. Challenge 2: power production from CO_2-rich stream

Given that CO_2 must be compressed to high pressures for efficient transport and storage, it would be inefficient to expand the CO_2-rich stream exiting from the GSC reduction stage to atmospheric pressure and then recompress it to the supercritical point. In the unabated plant, however, all process gases pass through the gas turbine to maximize efficiency.

This challenge can be mitigated by implementing a heat exchanger between the outlet gases from the GSC reduction stage and the inlet

gases to the oxidation stage as shown in Fig. 4. In this way, most of the high quality energy in the CO_2-rich stream is transferred to the air that passes through the gas turbine, maximizing the conversion efficiency to useful work.

Since the CO_2 stream is about 7 times smaller than the air stream, this effect is likely to be significantly smaller than the effect of the TIT discussed in the previous section. Even so, the potential efficiency gain is significant and will therefore be further investigated in this work.

2.3. Opportunity 1: exploitation of fuel HHV

In conventional combustion processes, it is not possible to exploit the fuel higher heating value (HHV) because the steam partial pressure in the combustion products is generally too low to condense at useful temperatures. Thus, plant efficiencies are normally given in terms of lower heating value (LHV).

The pressurized CO_2-rich stream exiting the GSC reduction stage contains steam at a much higher partial pressure – about 6 bar in the case of GSC-IGCC. This allows for most of the heat of condensation to be recovered in the economizer of the HRSG cooling the CO_2-rich stream, to an extent compensate for the fact that combustion products are not expanded in the Gas Turbine as in a conventional system

For coal, HHV is only about 4% higher than LHV, so the impact of this opportunity will be relatively small. This work will therefore not study this opportunity in detail, but only quantify the fraction of condensation enthalpy naturally recovered in the HRSG. When GSC is applied to NG or syngas from steam gasification, however, this opportunity increases substantially and more elaborate heat integration strategies may become beneficial to ensure maximum power production from the additional steam condensation enthalpy.

2.4. Opportunity 2: post-combustion gas clean-up

IGCC plants present the opportunity for efficient gas clean-up because pollutants (primary sulphur compounds) are concentrated in the syngas stream. If uncleaned syngas is combusted in air, the resulting SOx pollutants are diluted in a large quantity of depleted air, making post-combustion gas clean-up much more expensive.

However, pre-combustion gas clean-up results in a significant efficiency penalty because the syngas needs to be cooled down to lower temperatures in order to remove contaminants, and then preheated with HP water before feeding it to the turbine combustor system. The cooling is generally done by raising steam, implying that the transferred heat can only be employed for power production in the bottoming cycle and not the complete combined cycle. Near-commercial hot gas clean-up technology (Denton, 2014) can reduce this penalty to a certain degree, but still does not eliminate it.

GSC offers the opportunity for cost-effective post-combustion gas clean-up because sulphur compounds will remain concentrated in the outlet gases from the GSC reduction stage. This can avoid the need for syngas cooling and also exploit the heating value of sulphur compounds or, in the case of biomass gasification, tar compounds.

A key technological uncertainty in this regard is the behaviour of the GSC oxygen carrier when exposed to uncleaned syngas. Literature studies show that Fe-based oxygen carriers perform well with contaminants like sulphur compounds (de Diego et al., 2014) and biomass tars (Matthew et al., 2016). Dedicated studies with real syngas in a GSC reactor will be required to properly assess the attractiveness of this opportunity.

If the oxygen carrier can tolerate uncleaned syngas, the removal of pre-combustion clean-up can lead to significant efficiency gains (and capital cost reductions). This study will quantify the potential efficiency gain from not having to cool the syngas and estimate further efficiency gains from combustion of contaminants in the GSC reactors.

3. Methodology

3.1. Reactor modelling

In the present study, the different fluidized bed reactors are modelled as Continuous Stirred Tank Reactors (CSTRs), which is a reasonable assumption considering the excellent mixing behaviour of fluidized beds. Furthermore, it is assumed that thermal and chemical equilibrium is reached within the reactor. The former is generally easily achieved due to extremely fast particle-fluid heat transfer in fluidized beds, where the particle sizes are generally in the order of 100 µm. The latter is also a reasonable assumption for industrial scale reactors using oxygen carriers that are reasonably reactive. For example, the results of a recent experimental lab-scale study of GSC with ilmenite as oxygen carrier (Zaabout et al., 2017), as used in the present study, suggest that ilmenite is sufficiently reactive to avoid significant fuel slip in industrial scale reactors. Additionally, the simulated reactors are operated in such a way as to avoid excessive reduction of the oxygen carrier, thus avoiding reaction rate limitations when approaching full conversion.

3.1.1. Reactions

Ilmenite ore is considered as oxygen carrier in the GSC process. In this case, results from literature (Abad et al., 2011) suggest that the redox reactions can be approximated through four heterogeneous reactions. Eq. (1)–(3) take place primarily in the reduction stage, whereas Eq. 4 mainly takes place in the oxidation stage. All reactions will proceed until one of the reactants is consumed.

$$CH_4 + 4Fe_2O_3 \rightarrow 8FeO + CO_2 + 2H_2O \; R_1 = \frac{1}{\tau} N_{CH_4} N_{Fe_2O_3} \tag{1}$$

$$H_2 + Fe_2O_3 \rightarrow 2FeO + H_2O \; R_2 = \frac{1}{\tau} N_{H_2} N_{Fe_2O_3} \tag{2}$$

$$CO + Fe_2O_3 \rightarrow 2FeO + CO_2 \; R_3 = \frac{1}{\tau} N_{CO} N_{Fe_2O_3} \tag{3}$$

$$O_2 + 4FeO \rightarrow 2Fe_2O_3 \; R_4 = \frac{1}{\tau} N_{O_2} N_{FeO} \tag{4}$$

To obtain fast enough reaction rates, R, to ensure that chemical equilibrium is reached in the simulations, τ is set to 0.01. In the above equations, N_i, denotes the amount of species i present in the reactor.

3.1.2. Mole and energy balances

The ode15 differential-algebraic equation solver in Matlab is used to solve the following mole and energy balances in the reactor.

$$\frac{dN_{g,i}}{dt} = F_g^{in} y_{g,i}^{in} - F_g y_{g,i} + \sum_k s_{i,k} R_k \tag{5}$$

$$\frac{dN_{s,j}}{dt} = \sum_k s_{j,k} R_k \tag{6}$$

$$\left(\sum_i N_{g,i} C_{Pi} + \sum_j N_{s,j} C_{Pj} \right) \frac{dT}{dt} = \sum_i \left(F_g^{in} y_{g,i}^{in} h_{g,i}^{in} - F_g y_{g,i} h_{g,i} \right) + \sum_k R_k \Delta H_k^R \tag{7}$$

Eq. 5 expresses the gas phase species mole balance. The left-hand term expresses the rate of change of $N_{g,i}$, the holdup of gas species i. The first and second terms on the right-hand side represent the molar flowrates of i into and out of the reactor. The final term on the right-hand side is a source term due to the different reactions. The solids mole balance in Eq. 6 is similar to that of the gas species, except that there is no inflow or outflow of solids material in the gas switching reactors.

The energy balance in the reactor is solved in Eq. 7. The left-hand term represents the rate of change of enthalpy in the reactor, whereas the first two terms on the right represent the inflow and outflow of enthalpy with the inlet and outlet gases. The last term on the right is

due to the change of enthalpy during the reaction. Here, ΔH_k^R is the reaction enthalpy of reaction k at a reference temperature of 298 K. Temperature-dependent heat capacities and enthalpies are obtained from Stull and Prophet (1971) for the gas species and from Robie and Hemingway (1995) for the solids species.

Lastly, the total number of moles of the gas in the reactor is calculated from the ideal gas law, which is a reasonable assumption considering the high temperatures and moderate pressures in the reactors.

3.1.3. Initial, boundary and operating conditions

The inlet flow rate, compositions and temperature to the reactors change between the two GSC stages, reactor operating strategies and with the different power plant configurations considered. However, the reactor dimensions considered in the simulations (height of 6 m and diameter of 3.5 m) were chosen to yield a low fluidization velocity of 0.37 m/s to minimize particle attrition and elutriation, requiring 4 reactors to be in the reduction stage. More detailed reactor modelling and economic assessment studies will be required to optimize the reactors by maximizing the fluidization velocity and minimizing the reactor size while still achieving complete fuel conversion and minimal particle elutriation.

An average reactor voidage of 0.65 was assumed, with a density of 4000 kg/m^3 for the oxygen carrier particles, which resulted in a reactor pressure drop of about 4% of the inlet pressure as assumed in the process simulations (Table A4). The ilmenite oxygen carrier contains 33 mass-% Fe_2O_3 when completely oxidized and the rest inactive TiO_2 (Abad et al., 2011). To prevent slow reaction rates, which may cause fuel slip, the GSC is operated to never reduce more than 80% in mass of the active material in the oxygen carrier. On the other hand, the oxidation reactions are generally very fast and slip of the oxygen will not pose an issue to the process, therefore no such limit is considered for the oxidation of the oxygen carrier.

The reduction stage times are set to achieve a specified oxygen carrier utilization. The oxidation stage time is then set to an integer multiple of the reduction stage time to allow a cluster of reactors to deliver a steady output stream. This ratio ranged from 8 to 10 in this study, depending on the compositions and temperatures of the streams fed to the reactor during the air and fuel stages. This was done to minimize variations in the fluidization velocity when switching between stages. The total number of reduction and oxidation reactors therefore varied between 36 and 44. When a steam purge is performed between stages to reduce the mixing, the purge stage time is set equal to the reduction stage time, requiring 8 additional reactors.

When possible, a delay in the switch of the outlet valve, relative to the inlet valve, is employed to reduce the mixing between the stages, as demonstrated in a previous study (Cloete et al., 2015). However, such a delayed switch is not possible for cases using a steam purge because the outlet molar flow rates of the different stages differ substantially in these cases due to the slow steam feed rate. A delayed outlet switch will therefore cause unacceptable fluctuations in the flow rate delivered to the downstream processes.

3.1.4. GSC reactor behaviour

Fig. 2 shows the typical behaviour of the GSC process over an entire cycle. In the reduction stage (the first 222 s), the oxygen carrier is reduced by the fuel, producing carbon dioxide and steam. During this stage, the reactor cools down due to slightly endothermic reactions and the relatively cold fuel gases entering the reactor. In the subsequent oxidation stage, the oxygen carrier is oxidized by air and heated by the highly exothermic reaction. A large excess of air is provided to sufficiently cool down the reactor after the oxygen carrier is fully oxidized.

As shown in Fig. 2, the GSC concept poses two fundamental challenges that are not faced by conventional CLC technology: 1) temperature variations across the cycle and 2) some mixing of CO_2 and N_2 directly after the inlet gases are switched. Although temperature variations become small enough to not affect turbine performance when outlet streams of different reactors are mixed together (Cloete et al., 2015), the first challenge causes the average reactor outlet temperature to drop significantly below the maximum achievable reactor temperature, thus reducing the plant efficiency. As an example, if the TIT could be set to the 1200 °C maximum GSC temperature instead of the 1154.5 °C used in the base case (see Table A7), the plant efficiency would increase by 0.8%-points. The second challenge reduces the achievable CO_2 capture efficiency by about 6%-points (Cloete et al., 2015). Four strategies to mitigate these negative effects have been proposed in earlier works (Cloete et al., 2015, 2017):

1 Increased efficiency can be traded for reduced CO_2 capture efficiency by shortening the cycle time (see Fig. 7 in Cloete et al. (2015)).
2 Short cycles combined with a steam purge between oxidation and reduction can improve performance (see Fig. 10 in Cloete et al.

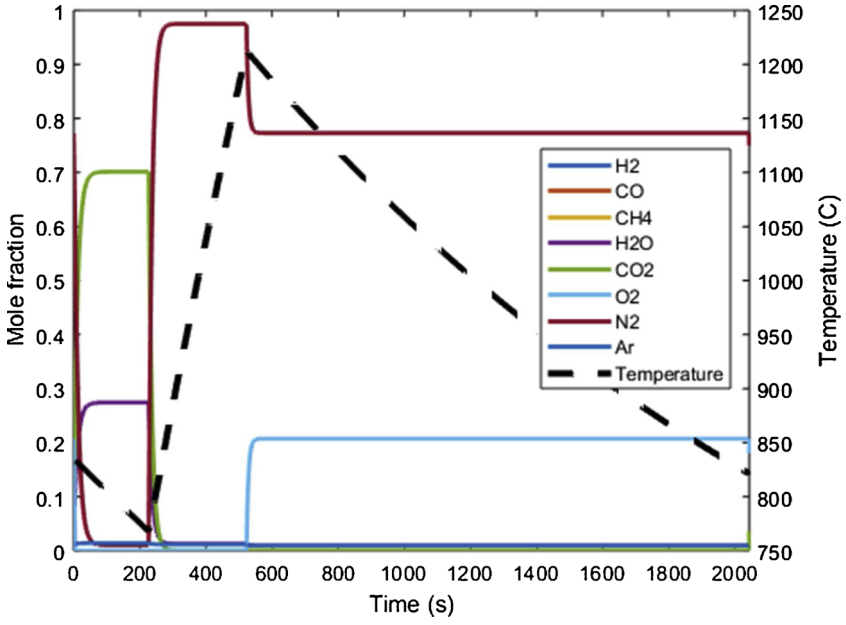

Fig. 2. Transient profile of species mole fraction and temperature over a typical GSC cycle.

(2015)). This strategy was simulated by inserting two additional steam stages when switching back and forth between fuel and air.

3 Further improvement is possible with an N_2 recycle stream to dilute the air going to the oxidation stage to limit the temperature variation when long cycles are used (see Fig. 12 in Cloete et al. (2015)). This strategy was simulated by combining a portion of the depleted air from the air stage with fresh air to form the feed to the GSC oxidation stage.

4 A concentrated injection of air into the reactor can limit O_2 conversion and thus replicate the effect of N_2 recycle (see Fig. 10 in Cloete et al. (2017)). This strategy was simulated by specifying a maximum degree of O_2 conversion in the GSC oxidation stage. This will be henceforward referred to as O_2 slip heat management strategy.

Strategy 3 is considered to be the best available option (Cloete et al., 2015) and will therefore be deployed in the cases where it is viable. However, this strategy is not possible in the cases with additional firing after the GSC reactors, where the outlet stream must contain enough oxygen to combust the additional fuel. In these cases, strategy 4 will be preferably employed. Strategy 2 will also be evaluated in the cases where strategy 4 had to be employed given that strategy 4 will complicate reactor design and may be challenging to implement in practice.

3.1.5. Link with process models

The inlet stream compositions and temperatures used in the reactor simulations are obtained from the process model, described in section 3.2. Selected output from the reactor model is then again provided as input to the process model. These steps are repeated as necessary to converge the results.

Output from the reactor simulations included the average temperatures from the reduction and oxidation stages and the fraction of mixing of the oxidation stage products into the reduction stage products. In case of steam purge, the steam purge output is included with the products from the preceding stage and the ratio of steam to air fed to the GSC reactor is specified to the process model.

3.2. Power plant modelling

The model of the power plant concept based IGCC and GSC technology was developed in Unisim Design R451, a powerful modelling tool for stationary process simulation developed by Honeywell. This flexible simulator allows integrating unconventional units such as the Gas Switching reactors (at average operating points) within the power cycle. The basic unit operation blocks also allow a simplification of complex process units such as syngas treating, whose auxiliary processes are less impactful from a power perspective. The Peng Robinson property method was employed to predict fluid properties across the flowsheet. A layout of the power plant is shown in Fig. 3.

3.2.1. Coal gasification

South African Douglas Premium bituminous coal is gasified in an entrained flow gasifier, Shell type, which requires pure oxygen as oxidizing agent and dry feed. A general overview of this gasification technology can be found in Higman and van der Burgt (2008). Coal flow rate is fixed as calculation basis. CO_2 from sequestration unit is provided at high pressure to the lock hoppers for coal loading. 10% of this CO_2 stream is vented to the atmosphere, while 70% is recirculated back to the CO_2 recompression unit. The remainder enters the gasifier with the coal feed. Oxygen with a purity of 95 mol-% is supplied by an air separation unit (ASU), consisting of a double column reboiler-condenser scheme with high pressure oxygen production by means of a liquid pump (Dawson et al., 2004). Liquid pumping of oxygen is preferred to a configuration with gaseous product compression for two main reasons, despite having a slightly higher specific power consumption: Oxygen compressors are a high cost critical equipment and generate special safety risks in that the compressor can burn violently. There is abundant literature dealing with optimal ASU design and integration with an IGCC plant (Han et al., 2017; Jones et al., 2011). However, because of the heat management strategies selected for the

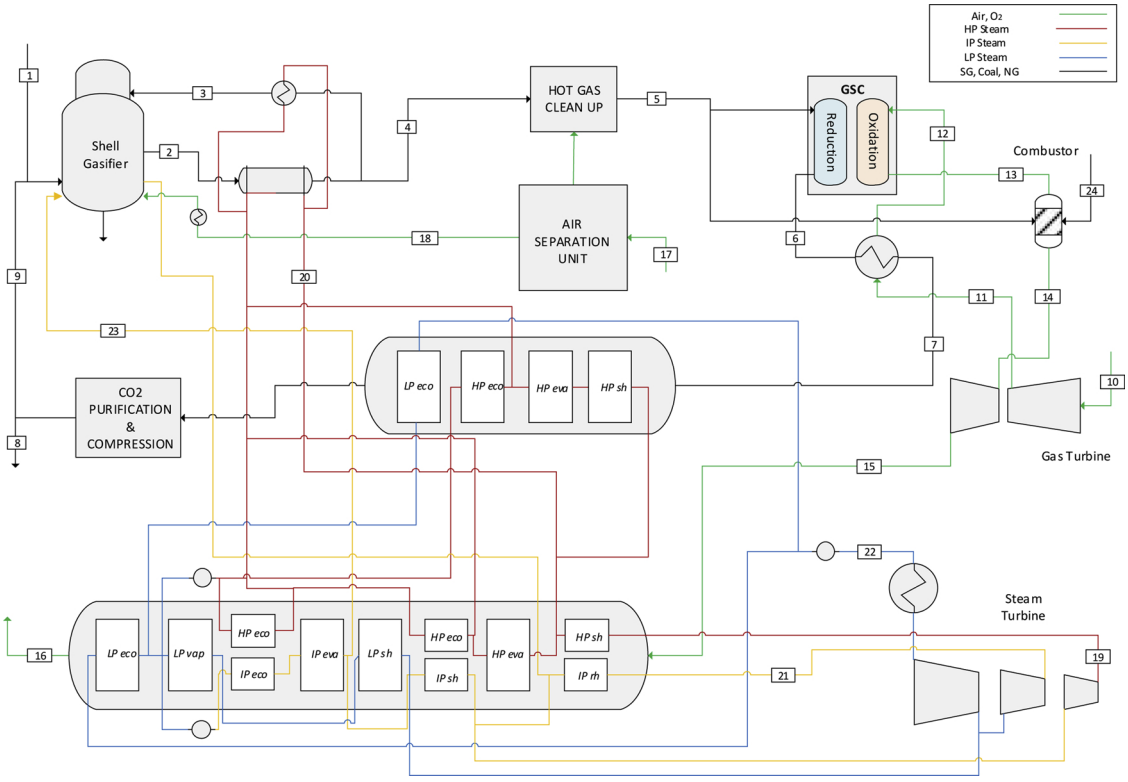

Fig. 3. Block Flow Diagram of the Power Plant Model with Extra Firing and GSC CO_2-rich outlet Heat Recovery.

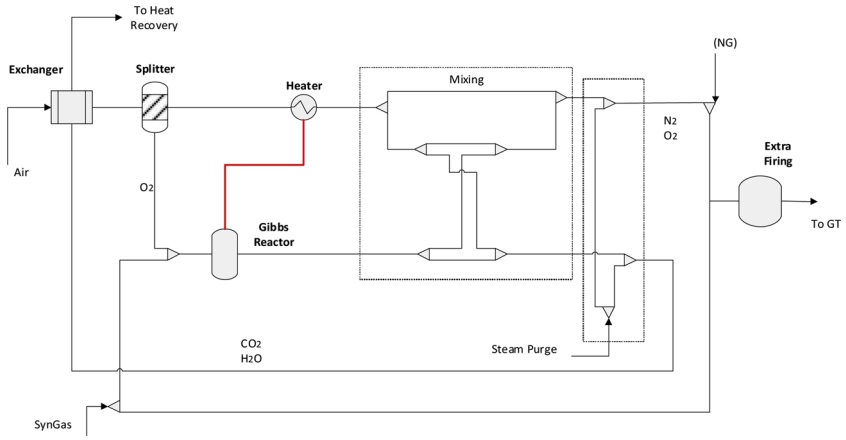

Fig. 4. Block Flow Diagram of the GSC model in Unisim with Extra Firing and CO_2-rich outlet Heat Recovery.

Gas Switching reactors (N_2 recycle) and for simplicity's sake, a standalone unit with no air side integration is selected, which facilitates plant start up and improves overall availability but with a higher auxiliary power demand and a dedicated air compressor in the unit.

Intermediate pressure steam (54 bar) generated in the Gasifier jacket is partially fed as moderator and partially used to heat up the oxygen inlet stream to 180 °C A partial quench-convective cooling configuration is chosen: the up flow gasifier operates at a high temperature (1550 °C) and the hot syngas is quenched to approximately 900 °C with cold gas at 300 °C from the syngas recycle compressor. A syngas effluent cooler (SEC) cools down the quenched syngas to reach 300 °C, performing as an economizer, evaporator and superheater of high pressure steam. In order to avoid metal dusting, the degree of superheating allowed in the syngas coolers was limited to 450 °C, carrying out the remaining superheat requirements in the heat recovery units downstream of the gas turbine. In this way, high tube temperatures in the more corrosive atmosphere at the top of the syngas cooler are avoided. The current upper limits of 139 MPa and 540 °C for steam come at a considerably higher cost (Zhu, 2015).

The granulated slag leaves the gasifier through a lock hopper system with water as continuous phase on the one hand, while the fly ashes entrained in the syngas are captured in a candle filter. Raw Syngas after the candle filter is split to provide the recycle stream for quenching and the remaining flow is sent to a scrubber (in the case of cold gas clean-up of syngas) to remove remaining particulate species; the syngas outlet temperature is around 160 °C.

The gasifier yields a high heating value syngas with a CO/H_2 ratio of approximately 3/1. Because of the high temperature of the gasifier, it is reasonable to assume a raw syngas composition determined by a thermodynamic equilibrium model. A high carbon conversion (> 99%) and Cold Gas Efficiency around 81% is achieved. Raw Syngas compositions are in line with parallel works on IGCC using a Shell gasifier and similar boundary assumptions. More detail of the Gasifier Island configuration which inspired this work can be found in Spallina et al. (2014). The main model parameters taken for the Gasifier Island are summarized in Table A1 in the Appendix A.

3.2.2. Syngas treating

This raw syngas leaving the gasification island undergoes a series of treatment processes to remove contaminants that would lead to harmful emissions downstream. The removal of sulphur species has been addressed with different configurations studied extensively in different works:

1 **Cold gas clean-up (CGCU)**: Syngas after the scrubber is heated to 180 °C and fed to a Carbonyl sulphide (COS) hydrolyser, which converts this species to hydrogen sulphide (H_2S) enhancing sulphur removal. The outlet of this conversion unit is cooled down to low temperature (35 °C) in a low pressure water economizer and routed to an acid gas removal unit (AGR). A physical selective absorption process known as Selexol unit achieves 99% sulphur removal. Physical absorption is favoured against chemical absorption due to the high selectivity of H_2S over CO_2, minimizing the presence of CO_2 in the acid gas, and consequently reducing the cost and size of the downstream SCOT and the Claus units. In the latter, H_2S is transformed to elemental sulphur, reaching an overall sulphur recovery of 999%. Auxiliary electrical consumption and absorbent regeneration duty are particularly low for this solvent and have been estimated in alignment with previous works. Power Plant schematics with cold gas clean-up reproduced in this work correspond to the configuration shown in Fig. 1 of Cloete et al. (2015).

2 **Hot gas clean-up (HGCU)**: In this configuration, removal of sulphur takes place at a high temperature, by means of adsorption beds with zinc oxide material. A system with two circulating fluidized beds (desulphurizer and regenerator) is employed. The following simplified chemical reactions take place:

$$\textit{In the adsorption bed: } ZnO + H_2S \rightarrow ZnS + H_2O \tag{8}$$

$$\textit{In the regeneration bed: } ZnS + \frac{3}{2} O_2 \rightarrow ZnO + SO_2 \tag{9}$$

In the regeneration step, which is not simulated here, compressed air is diluted with nitrogen available from the ASU at sufficient pressure in order to reduce the partial pressure of oxygen in the regeneration stream, preventing the occurrence of undesired reactions which form zinc sulphate. This species reduces the adsorbent capacity and potentially transfers oxygen molecules to the adsorption stage (where they are released and combust the syngas). The regenerator outlet containing SO_2 is expanded after being filtered and routed to a wet flue gas desulphurization unit (WGFD). A moderately low desulphurization temperature of 400 °C was selected, well below 650 °C where ZnO is reduced to Zinc and volatizes. Previous studies show a relatively small influence of hot desulphurization temperature on the thermal efficiency of the plant (Giuffrida et al., 2013, 2010).Thus, the desulfurization temperature should be selected mainly on the basis of both technical and economic considerations. Syngas after clean-up is filtered to avoid adsorbent particulate material entering the GSC reactors. Since no scrubber is present in this configuration, other sorbents should be used to remove trace contaminants (HCN, HCl, NH_3 etc.) as described in Ohtsuka et al. (2009). The latter have no detrimental effect on ZnO capacity to remove H_2S.

3 **Post-combustion gas clean up**: In this configuration it is assumed that H_2S is combusted in the GSC reactors to deliver a reduction gases stream with SO_2. Although the sulphur heating value is utilized in the topping cycle and inefficiencies due to syngas cooling are avoided, the presence of SO_2 can lead to corrosion issues (Kim and Lee, 2014) in the heat recovery unit and affects the quality (and end use) of the captured CO_2 stream. SO_2 could be geologically stored with CO_2 which may even reduce costs if corrosion issues (primarily related to the presence of water) can be avoided (Gimeno et al., 2018). Alternatively, a scrubbing technology (Srivastava et al., 2001) could be employed to achieve a SO_2 recovery above 95% with minimal impact on plant efficiency, but increased capital cost. Given the possibility to store SO_2 with CO_2 and the minimal impact of SO_2 scrubbing on plant efficiency, the desulphurization of the CO_2 stream however was not modelled in the present work.

The main process assumptions for syngas treating are summarized in Table A2 in the Appendix A.

3.2.3. Gas switching combustion simulation

After syngas is freed from contaminants, it is heated up to 300 °C with HP hot water and then fed to the GSC reactor system in case CGCU is used. When HGCU is chosen, syngas is fed at the highest available temperature to the reactors. No syngas dilution with reduced gases from the reactor outlet is necessary when using fluidized reactors. The good mixing properties achieved in the fluidized bed, whose reactor model could be represented as a continuous stirred tank reactor (CSTR), prevent potential carbon deposition on the carrier.

The transient nature of the gas switching technology is not reflected on the power plant simulation. Instead, a stationary simulation with average reactor temperatures and total stream flow rates represents the cluster of reactors by means of a Gibbs reactor and a heater, as shown in Fig. 4. For a given GSC oxidation temperature, correlations have been derived from a set of reactor simulations carried out following the methodology described in Section 3.1, that determine the difference in average temperature between oxidation and reduction stages and the fraction of mixing between streams. For cases with steam purge as heat management strategy, the correlations determine the required IP superheated steam that must be introduced in order to achieve a desired amount of mixing. IP Superheated steam was chosen for two reasons: 1) avoid extra complexity in the heat recovery units by introducing a different pressure level and more importantly 2) a high steam temperature minimizes potential undesired temperature gradients along the cycles of the oxygen carrier.

When extra firing cases are simulated, an additional combustion chamber is required. A fraction of the syngas outlet from the HGCU is fed to this unit. Alternatively, pipeline natural gas (Altfeld and Schley, 2012) can be also used as fuel. It is assumed that natural gas is available at sufficient pressure and undergoes no pre-treatment or preheating before entering the combustion chamber, see detailed specifications in Table A4 in the Appendix A. The flow rate required in each case is determined by the oxidation temperature of the GSC and the TIT (combustor outlet) which was specified to a value of 1360 °C, that of an advanced unabated IGCC gas turbine (Cloete et al., 2015). Fig. 4 shows a diagram with the basic block model for GSC in Unisim with extra firing and heat recovery from GSC reduction stage outlet. The stream mixing and steam purge are modelled by a series of mixing and splitters at reactor outlet.

For extra firing cases with NG, the coal flow rate as calculation basis remained unchanged. Therefore, the bigger thermal input increases the size of the power plant substantially as can be seen in the Appendix A summary Table A7. Gas turbine size will be the equipment limiting the size of the plant. Coal flow rate could be adjusted to reach a specified gas turbine(s) power output(s), making gasifier, ASU and Clean-Up units smaller. GSC and Extra Firing model parameters can be found in Table A4 in the Appendix A.

3.2.4. CO_2 purification unit

Although GSC concept intends to provide an inherent separation of the combustion gases from air, a certain mixing between the gaseous streams is unavoidable as a consequence of the switching valve mechanism. A purification unit is necessary to increase the CO_2 concentration from approximately 92 mol-% after drying (this concentration depends on GSC operating conditions like cycle length, air to fuel ratio, etc.) to a concentration of at least 96 mol-%, which is the typical boundary specification for cost-effective CO_2 transport (Kolster et al., 2017).

The CO_2 purification unit (CPU) process line up is similar to the one described in Campanari et al. (2016). Firstly, this stream is cooled down to ambient temperature knocking out all condensed water. It is further compressed in a first stage compressor, subsequently cooled and finally undergoes a drying stage. A refrigeration unit with a two temperature flash vessel is the method employed to carry out the purification of this stream. The dried stream is cooled down and flashed in the high temperature vessel. The operating temperature of the first flash is fixed to −33 °C. The liquid outlet of this vessel is throttled and provides cold to the cryogenic heat exchanger cooling the feed to the unit, the valve discharge pressure is set to achieve an assumed minimum temperature approach in the heat exchanger. The gas outlet from the high pressure vessel, rich in lighter components such as nitrogen, is further cooled and flashed in the low temperature flash vessel. Again the liquid outlet stream is throttled to a low pressure after receiving some heat (the pressure is determined by the lowest temperature possible while avoiding CO_2 freeze out) and cools the inlet feed. The gaseous stream, which constitutes the purge from the unit, has a relatively small flow rate and is comprised mainly of nitrogen and some CO_2. This stream undergoes a series of heating and expansion cycles: it absorbs heat from the inlet streams to the vessels and is subsequently expanded and cooled down again. Three expansion-reheating cycles are necessary to discharge this stream at near ambient temperature and pressure. Such expansion steps generates valuable work that can be discounted from the CO_2 recompression requirements. Since the purge flow rate is low, this retrieved duty is relatively small however. Inevitable CO_2 losses are inherent to this purification method and depend to a large extent on the unit inlet composition, but the purification efficiency i.e. the fraction of retained carbon, is generally above 96% for inlet compositions above 85 mol-% of CO_2.

In all CPU simulations, the CO_2 solidification line has not been surpassed in order to avoid dry ice formation that would potentially block heat exchangers by limiting the outlet temperatures of valves and expanders to −56 °C. Process parameters and equipment efficiencies for this unit can be found in Table A3 in the Appendix A.

3.2.5. Power generation from combined cycle

The hot depleted air coming out from the GSC oxidation stage is expanded in the gas turbine, delivering work to a generator. The outlet stream, at a temperature somewhat below 500 °C, is routed to a heat recovery steam generator (HRSG) unit. This unit consists of a two steam pressure level with reheat heat recovery system based on the configuration shown in Cloete et al. (2015).

Because of this low turbine outlet temperature (TOT), the superheating of the HP steam and IP reheating is mainly done in a second heat recovery unit that takes advantage of the enthalpy contained in the reduction gases outlet stream. In such a configuration, with high temperatures available for steam superheating (> 1000 °C) and a significantly high flow rate of HP steam from the SECs, the difference in steam cycle efficiency between 2 and 3 pressure levels with reheat is relatively small as shown by Kehlhofer et al. (2009). In the cases where N_2 recycle is chosen as heat management strategy, the HRSG outlet is further cooled from the stack outlet temperature (which is case dependent and limited to a minimum of 80 °C) to 25 °C and recycled to the air inlet compressor.

For the cases where extra firing is done and CO_2 rich outlet heat is

recovered by the air stream in an exchanger, a different steam production layout is needed. A reconfigured HRSG unit (3 pressure levels with reheat) for the depleted air gas turbine outlet at around 600 °C was designed, with similar parameters as Kotowicz and Brzęczek (2018). The superheaters of the CO_2 rich outlet from GSC in the heat recovery unit are removed, because of the lower temperature (470 °C) of this stream after the heat exchanger.

Due to the large number of simulations carried out, pressures levels were fixed to a certain reference value, and although a further slight optimization of these levels could be possible, a like for like comparison can be shown between the cases. Steam cycle improvement and optimization is a scope of future detail work for the IGCC gas switching concepts which show the most promising results. All the model assumptions of steam and gas turbine, as well as HRSG units are given in Table A6 in the Appendix A.

3.2.6. Simulation cases

In view of the efficiency enhancement opportunities described in the introduction chapter, the summary of the cases selected for simulation is shown in Table 1.

A schematic of the power plant for the extra firing case with hot gas clean up, CO_2-rich outlet heat exchanger recovery and the above-mentioned heat steam recovery generator units is depicted in Fig. 3. A stream summary for the most efficient case E2 is included in Table A8 the Appendix A.

4. Results and discussion

Results will be presented in seven sections. Firstly, a sensitivity analysis varying the maximum GSC temperature was performed for the Base Case and D1 case. The efficiency trade-off with decreasing TIT and alternatively, the emissions increase due to a larger fraction of syngas being fired in the combustion chamber to maintain a constant TIT, are obtained. Secondly, the effect of hot gas clean-up will be briefly presented together with the effect of different GSC heat management strategies. The next four sections will then present results quantifying the efficiency enhancements that may be expected from exploiting the two opportunities and overcoming the two challenges discussed in Section 2. Finally, a best case scenario will be presented to illustrate the potential efficiencies that can be achieved by a GSC-IGCC plant.

4.1. Sensitivity analysis on maximum GSC temperature

In order to assess the uncertainty related to operational challenges of oxygen carrier materials, valves and filters at elevated temperatures, a sensitivity analysis for three different maximum GSC operating temperatures (1000, 1100 & 1200 °C) was performed. The evaluation was carried out for the base case topology and for the case with syngas extra firing with heat exchanger recuperator (case D1). With the purpose of maintaining a reasonable performance of the steam cycle in the base case (achieving sufficient steam superheat) the pressure ratio had to be reduced to 15 and 10 for maximum GSC operating temperature of 1100 and 1000 °C respectively. The polytropic efficiency of the turbine remained constant throughout the cases.

Fig. 5 shows that a decrease in the maximum reactor temperature has a large negative influence on the plant performance, causing an efficiency drop of 6.7%-points. As a consequence of lower operating pressure, reduced mixing of gases when switching between oxidation and reduction leads to a slight improvement in the CO_2 capture performance (1.6%-points).

For the case with extra firing, lowering GSC operating temperatures requires a larger portion of syngas to be combusted in the firing chamber, increasing the plant emissions significantly (23.8%-points reduction in CO_2 capture). Because a slightly higher flow rate is sent to the gas turbine (syngas combustion products) and lower auxiliary power is required to compress captured CO_2, the plant efficiency improves by 0.9%-points as GSC temperature decreases, as shown in Fig. 5.

These results clearly illustrate the importance of maximizing the GSC operating temperature. Achieving a maximum temperature of 1200 °C may require the use of a more expensive oxygen carrier such as the NiO-based material that was shown to fluidize well at temperatures close to 1200 °C by Kuusik et al. (2009). The gentle fluidization in GSC reactors will minimize particle attrition to maximize oxygen carrier lifetime, thereby limiting the economic impact of using more expensive materials. Subsequent cases will therefore assume that such high temperature oxygen carriers will be available by the time that CLC becomes a commercial technology, allowing for a maximum GSC temperature of 1200 °C.

4.2. General GSC-IGCC efficiency strategies

Hot gas clean-up (HGCU) is a well-known strategy for enhancing IGCC efficiency. As shown in Fig. 6, the inclusion of HGCU technology increases the GSC-IGCC efficiency by 1.1%. This is significantly less than an earlier work (Giuffrida et al., 2010) where HGCU technology for an unabated IGCC power plant is investigated. Giuffrida et al. (2010) used two gas turbine units, resulting in a relative duty from topping to bottoming cycle of approximately 1.6, whereas this ratio is 0.9 in the present work for the reference case (one gas turbine to one steam turbine unit). This is mainly because GSC technology delivers the reduction gases separately from air and these gases are therefore not expanded in the gas turbine. The enthalpy of this stream is invested entirely for additional steam production. Thus, the GSC configuration presents a steam cycle to gas turbine duty ratio substantially bigger to that of a conventional unabated IGCC. Compared to an earlier study (Cloete et al., 2018a), which uses similar GSC technology (packed bed configuration) instead of the gas turbine combustor, the efficiency benefit from HGCU technology is about half because the present study delivers a smaller syngas flowrate (with a higher heating value).

The case with cold gas clean-up returns a very similar efficiency to previous simulations of the GSC-IGCC process (Cloete et al., 2015), allowing that study to be used as a benchmark. In subsequent cases, hot gas clean-up will be used as the default because this technology is near commercial readiness and will almost certainly be available by the time that GSC-IGCC plants are commercialized.

The cases investigating gas clean-up technology were carried out with the default N_2-recycle heat management strategy. A case achieving a similar CO_2 capture ratio using the steam purge strategy was also completed for perspective. As expected, Fig. 6 shows that this strategy is less efficient, imposing a penalty of 1.4% relative to the N_2-recycle strategy. All cases show an attractive CO_2 capture ratio reaching 93%.

Table 1
Simulation Cases Overview.

Case	Syngas Treating	GSC Operation	Extra Firing	
			Type	Heat Recovery
Base Case	HGCU	N_2 recycle	No	–
A1	CGCU	N_2 recycle	No	–
A2	HGCU	Steam Purge	No	–
B1	No Treating (900 °C)	N_2 recycle	No	–
B2	No Treating (1200 °C)	N_2 recycle	No	–
C1	HGCU	O_2 slip	Syngas	No
C2	HGCU	Steam Purge	Syngas	No
C3	HGCU	O_2 slip	NG	No
C4	HGCU	Steam Purge	NG	No
D1	HGCU	O_2 Slip	Syngas	Yes
D2	HGCU	Steam Purge	Syngas	Yes
D3	HGCU	O_2 slip	NG	Yes
D4	HGCU	Steam Purge	NG	Yes
E1	No Treating (900 °C)	O_2 slip	Syngas	Yes
E2	No Treating (900 °C)	O_2 slip	NG	Yes

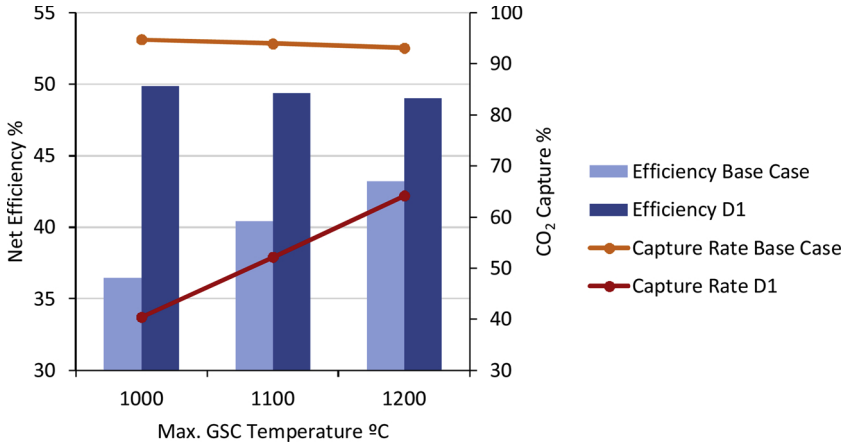

Fig. 5. Sensitivity analysis of maximum GSC operating temperature on plant net efficiency and capture rate for Base Case and D1 case.

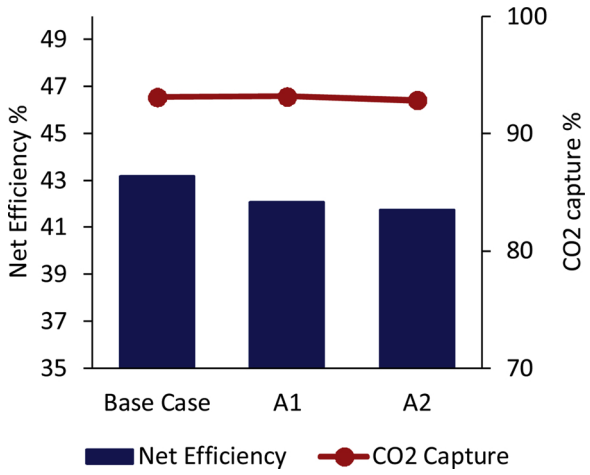

Fig. 6. Electric efficiency and CO_2 capture ratio for four different GSC-IGCC configurations. Case numbering is detailed in Table 1.

4.3. Post-combustion gas clean-up

Eliminating pre-combustion gas clean-up removes the need for syngas cooling. However, syngas is still quenched after exiting the gasifier at a temperature of 1550 °C. Two quench temperatures are evaluated in this study: 1200 °C (the maximum GSC temperature), which requires modification of SEC to withstand such temperature, and 900 °C, the default quench outlet temperature of the gasifier which avoids to an extent technology challenges with syngas filters (Heidenreich, 2013). Fig. 7 shows that avoiding pre-combustion gas clean-up achieves a 1.1% efficiency gain over the default case with HGCU. However, no substantial efficiency improvement was obtained for a syngas temperature of 1200 °C.

The GSC reactor outlet temperature is also enhanced by an increase in the inlet fuel temperature because the temperature drop under reduction (see Fig. 2) will be smaller. As a result, the TIT of the case with 900 °C and 1200 °C syngas temperature was 1164 °C and 1179 °C respectively, relative to 1154 °C for the base case with HGCU, creating a small additional efficiency gain. Furthermore, the removal of the gas clean-up units results in lower auxiliary power consumption, amounting to approximately 0.15% for the HGCU case.

Although higher syngas temperatures for a fixed GSC outlet temperature lead to larger flowrates and temperatures to the gas turbine, the extra duty delivered by the gas turbine is compensated by the lower amount of HP steam that can be produced in the SECs when less syngas cooling is required. Due to a lower HP steam flow rate, the steam turbine output decreases. To illustrate this point, the power breakdown for the three cases is shown in Fig. 8 (left), while the different flow rates for HP steam from SECs, total steam flow and N_2 flow to the GT are plotted in Fig. 8 (right). Because of a higher flow rate to the HRSG as syngas temperature increases, the overall steam flow rate of the cycle decreases mildly, as opposed to the large decrease observed for high energy quality HP steam from the SEC's. This bigger flow rate in the HRSG cannot convert water to HP steam as effectively as the syngas coolers, where much higher temperatures are available for that purpose.

Removal of pre-combustion gas clean-up can also allow the GSC process to fully exploit the heating value of syngas contaminants. For coal, about 1% additional heating value can be expected from 1.5 mass-% sulphur content if all sulphur is present as H_2S in the syngas. Biomass would present a larger opportunity in this regard where efficient utilization of tars can increase the syngas heating value by about 4% (Huang et al., 2011). This implies that contaminant combustion can potentially result in about 0.5%-points of efficiency gain for coal and 2%-points for biomass.

4.4. Utilizing fuel HHV

The fraction of steam in the CO_2-rich stream that is successfully condensed in the HRSG is close to 70%. This represents, for the base case, approximately 18 MW of additional heat that is upgraded in the HP and LP economizers of the CO_2-rich stream heat recovery unit. It is difficult to estimate the efficiency with which this added heating value

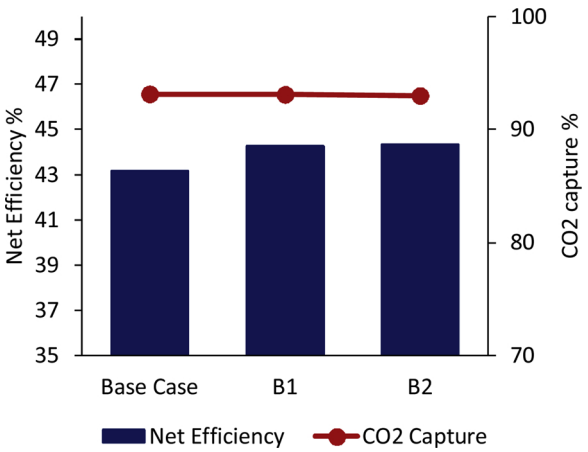

Fig. 7. Electric efficiency and CO_2 capture ratio for of cases without pre-combustion gas clean-up compared to the base case with HGCU. Case numbering is detailed in Table 1.

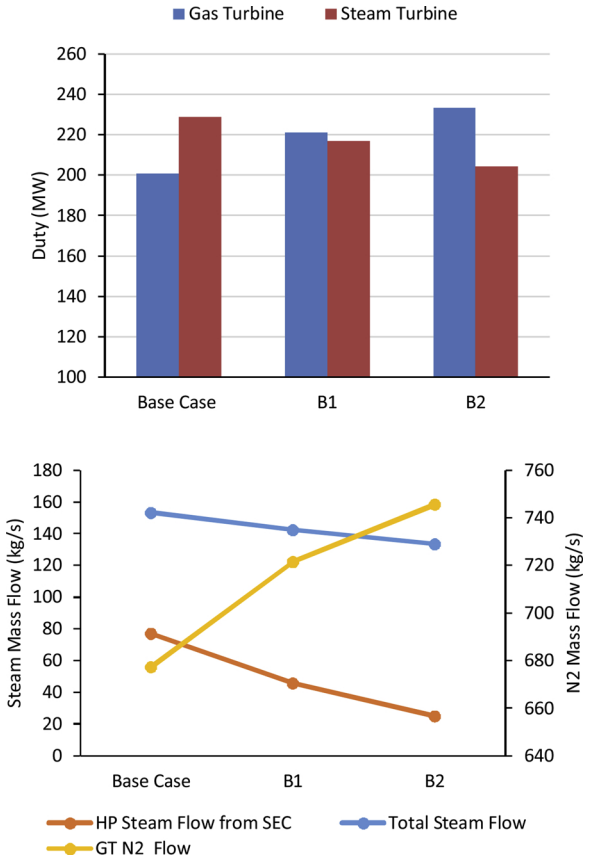

Fig. 8. Power breakdown (above) and stream flows (below) for the reference and post combustion gas clean-up cases. Case numbering is detailed in Table 1.

is converted to electricity, but the final efficiency gain is probably less than 1%-point (8.5 MW for the plant scale adopted in this work) of LHV fuel input.

It is important to note that, even though this gain is relatively small, it happens naturally in the GSC-IGCC plant without the need for process modification. This inherent efficiency gain cancels out most of the unavoidable efficiency loss of having to compress CO_2 for transport and storage.

4.5. Additional firing after GSC

Four cases with additional firing to raise the GSC reactor outlet temperature were completed: two with syngas firing and two with NG firing. Compared to the base case, Fig. 9 shows that additional firing results in large efficiency gains (maximum of 3.7%-points for syngas and 5.2%-points for natural gas), but also lower CO_2 capture ratios (67.8% and 82.4% respectively). The O_2-slip heat management strategy improves the efficiency by about 0.5%-points relative to the simpler steam purge strategy.

Firing with NG shows a 1.5%-point efficiency increase relative to syngas, mainly because NG does not experience the efficiency losses related to coal gasification and syngas cleaning. In addition, firing with NG shows a clear increase in CO_2 capture ratio. This occurs because of the higher H_2 to C ratio of this fuel (2 to 1) compared to syngas (1 to 3). The natural gas efficiency gain of 5.2%-points from 18.5% of the fuel LHV input fed to the combustor in the present study is comparable to the 3%-point increase from 10% of the fuel fed to the combustor by Zerobin and Pröll (2017).

Despite the decrease in CO_2 capture ratio, additional firing with carbon-containing fuels eliminates most of the 5.7%-point energy penalty of GSC-IGCC relative to an unabated IGCC plant with the same TIT evaluated earlier (Cloete et al., 2015). Further work is required to estimate the effect of integrating H_2-production with integrated CO_2 capture to maximize the CO_2 capture ratio.

4.6. Efficient power production from CO_2-rich stream

As shown in Fig. 10, implementing a heat exchanger (recuperator) between the reduction stage outlet and oxidation stage inlet gases increases the efficiency by an extra 2.1%-points and 1.9%-points for syngas and natural gas respectively. The most efficient cases for extra firing and syngas without CO_2 rich stream heat recovery are shown for perspective. The CO_2 capture ratio decreases by 1.7–3.4 %-points because a larger air flowrate must now be heated from the GSC outlet temperature to the TIT, and consequently a larger fraction of syngas and a higher flow rate of natural gas are required in the extra firing combustion chamber. Note that this case with the exchanger could only be evaluated with additional firing because a sufficiently high TOT (600 °C) is now available to superheat the steam in the HRSG that would otherwise have been superheated by the CO_2-rich outlet stream.

The combined efficiency gain from additional syngas firing and heat exchange amounts to 5.8%-points, which exactly eliminates the 5.7%-point energy penalty of the basic GSC-IGCC configuration. Utilizing natural gas instead of syngas as the extra firing fuel results in an even greater total efficiency gain of 7%-points. It should be noted, however, that a similar efficiency gain would be observed in the unabated IGCC benchmark plant if the same fraction of NG was added to the syngas.

The O_2 slip heat management strategy improves the efficiency by 1% with respect to steam purge, as a result of increased air flow rates for the cases with CO_2-rich stream heat recovery that leads to increased steam consumption to reach similar carbon capture ratios.

4.7. Maximum achievable efficiency

As shown in Fig. 11, the highest achievable efficiency from the GSC-IGCC configuration is 49.6% and 50.9% when using additional syngas and NG, respectively, for firing. This is much higher than the 41.6% efficiency of the original GSC-IGCC configuration and even substantially higher than an unabated IGCC plant at 47.3% efficiency (Cloete et al., 2015). When the TIT is raised from 1155 °C to 1360 °C the effect of post combustion gas clean-up (with respect to of HGCU, cases D1 & D3) is reduced to an extra 0.6% and 0.7% for syngas and natural gas respectively. This is a consequence of a reduced HP steam generation in the bottoming cycle when the energy in the rich CO_2 stream is transferred to air though the recuperator, as opposed to raising and superheating HP steam. An additional case for natural gas firing was run with post combustion clean-up and syngas at a temperature of

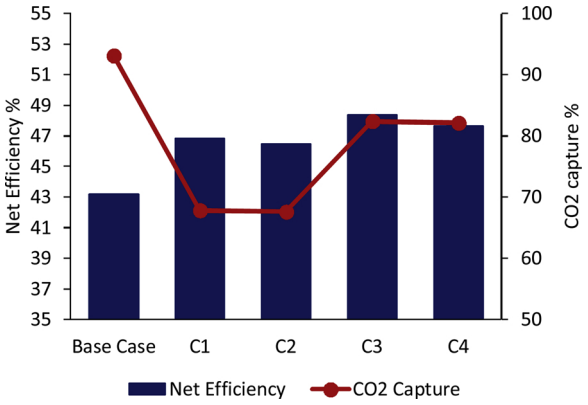

Fig. 9. Electric efficiency and CO_2 capture ratio for four different additional firing options compared to the reference case. Case numbering is detailed in Table 1.

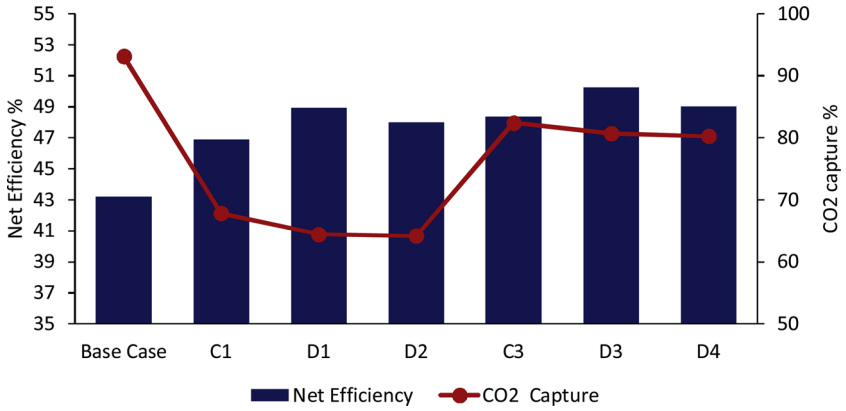

Fig. 10. Electric efficiency and CO_2 capture ratio for cases with and without heat exchange between the reduction outlet and oxidation inlet gases. Case numbering is detailed in Table 1.

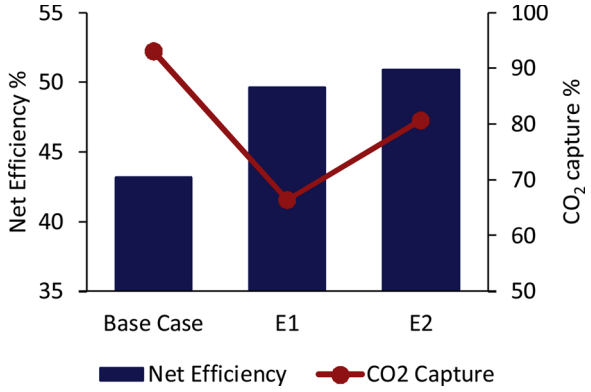

Fig. 11. Electric efficiency and CO_2 capture ratio for the most efficient configurations using additional NG and syngas firing. Case numbering is detailed in Table 1.

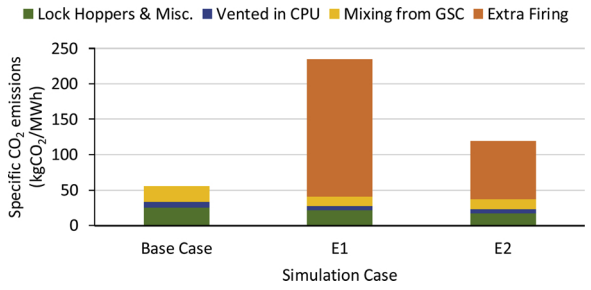

Fig. 12. Specific CO_2 emission breakdown for the base case and the two most efficient options. Case numbering is detailed in Table 1.

1200 °C, which resulted in a slight loss of efficiency with respect to the case with syngas temperature of 900 °C.

Due to the combustion of carbon-containing fuel after the GSC reactors, the CO_2 capture ratio drops to 66.4% and 80.7% for syngas and natural gas respectively. However, since the efficiency is significantly higher than the unabated benchmark plant, CO_2 avoidance will actually be higher than the CO_2 capture ratio.

As discussed in Section 2.1, such a highly efficient partial capture plant can be constructed during times with limited CO_2 pricing and retrofitted to fire with H_2 if the CO_2 price becomes very high. In such a case, H_2 dilution with nitrogen from the ASU is a possibility to avoid high flame temperatures that produce NOx emissions in gas turbines. Process integration of H_2 production units based on gas switching technology will be the subject of future investigations. Fig. 12 shows the specific CO_2 emission breakdown for the cases shown in Fig. 11. Although the syngas fraction routed to extra firing is approximately 25%, and the LHV thermal input of natural gas represents around 21% of the total, CO_2 emissions from extra firing for syngas and natural gas results in 82% and 69% of the total plant emissions respectively. This illustrates the attractiveness of H_2 firing to curtail this source of emissions.

In the case where extra firing is done with syngas with post-combustion clean-up, it is noteworthy to mention that only the sulphur components in the syngas fed to the GSC reactors will be efficiently captured. Sulphur in the syngas fed to the additional combustor will greatly increase the SOx emissions of the plant. In this case, the option of additional firing with natural gas clearly becomes more attractive than additional firing with syngas.

As gas turbine technology improves, the TIT can potentially be increased beyond 1360 °C to further boost the efficiency. This will increase the relevance of additional firing after the GSC reactors and therefore also the importance of integration of an efficient H_2-production process for additional firing without CO_2 emissions. More detailed power cycle optimization studies also have the potential to unlock significant further efficiency gains, especially given the limitations related to HP steam generation encountered in the cases with post-combustion gas clean-up.

Finally, the potential of GSC-IGCC to integrate a gas switching oxygen production (GSOP) process, as was done earlier for packed bed reactors (Cloete et al., 2018a), should also be acknowledged. GSOP can avoid most of the ~4%-point energy penalty imposed by the ASU in the GSC-IGCC power plant, offering significant additional plant efficiency at a cost of added plant complexity. The effect of the efficiency enhancements discussed in this work on a power plant replacing the ASU with GSOP reactors will be the topic of future study.

5. Summary and conclusions

Gas switching combustion (GSC) is a promising technology for accelerated scale-up of CCS power plants with minimal energy penalty. Even though initial power plant simulations of GSC integrated into an IGCC power plant clearly outperformed first-generation pre-combustion CO_2 capture, the energy penalty relative to an unabated benchmark IGCC plant remained significant (5.7%-points). This work investigates four ways to further improve the efficiency of the GSC-IGCC power plant with the aim of exceeding the efficiency of an unabated IGCC benchmark.

The energy penalty imposed by GSC-IGCC stems from two main challenges: 1) the reactor cannot reach the operating temperature of modern gas turbines and 2) work can only be recovered from the CO_2 stream via the bottoming cycle. The first challenge can be overcome by

Table A1
Gasifier Island Model Assumptions.

Air Separation Unit		
Equipment/Item	***Value***	***Units***
Polytropic Efficiency Compressor Stage	90	%
Expander Isentropic Efficiency	87	%
Reboiler-Condenser Pinch	2	ºC
Heat Exchanger Minimum Approach Temperature	2	ºC
Process Stream Temperature after heat rejection	25	ºC
Oxygen Purity	95	%
Oxygen Pressure	45	bar
Oxygen Pump Efficiency	80	%
Exchanger Pressure Losses / side	10	kPa
Intercooler Pressure Loss	10	kPa
Gasifier		
Equipment/Item	***Value***	***Units***
Moderator (steam) to coal ratio	0.09	kg/kg
Oxygen to coal ratio	0.9	kg/kg
Moisture in Coal Inlet to Gasifier	2	%
Fixed Carbon Conversion	99.3	%
Gasifier Operating Pressure	44	bar
Steam Moderator Pressure	54	bar
Oxygen to Gasifier Temperature	180	ºC
Heat Loss as % LHV	0.7	%
Balance of Plant as % LHV	0.15	%
CO_2 HP/HHP Pressure	56/88	bar
CO_2 Temperature	80	ºC
CO_2 to Dry Coal ratio	0.83	kg/kg
Coal Milling & Handling	100	kJ/kg coal
Ash Handling	50	kJ/kg ash
HP Water for Syngas Drying	2900	kJ/kg H_2O
CO_2 vented in Lock Hoppers	10	%
CO_2 recycled to Recompression	70	%
Syngas Quench & Convective Cooler		
Equipment/Item	***Value***	***Units***
Quenched Syngas Temperature	900	ºC
Cold Recycle Gas Temperature	300	ºC
Recycle Fan Polytropic Efficiency	80	%
Recycle Fan Mechanical Efficiency	92	%
Syngas Effluent Cooler Pressure Drop	4	%
Syngas Effluent Cooler Heat Loss	0.7	%
Superheat Steam Temperature in SEC	450	ºC

Table A2
Syngas Treating Modelling Assumptions.

Cold Gas Clean Up		
Equipment/Item	***Value***	***Units***
Syngas Temperature at Absorption Column	35	ºC
Heat Duty LP Steam to Regenerator	20.95	MJ_{th}/kg H_2S
Electric Consumption	1.93	MJ_e/kg H_2S
Hot Gas Clean Up		
Equipment/Item	***Value***	***Units***
Syngas Temperature at Adsorption Bed	400	ºC
Electric Consumption of Auxiliaries	5.34	MJ_e/kg H_2S

Table A3
CPU Modelling Assumptions.

CO_2 Purification Unit		
Equipment/Item	***Value***	***Units***
Compression Stages	3	–
Intercooler Pressure Drop	10	kPa
Process Stream Temperature after Heat Rejection	25	ºC
Exchanger Minimum Temperature Approach	2	ºC
Exchanger Pressure Loss / side	10	kPa
Compressor Stage Isentropic Efficiency	80	%
Expander Stage Isentropic Efficiency	85	%
Minimum Cold Stream Temperature	−56	ºC
Flash Vessels Temperatures HT/LT	−33/-53	ºC
Mechanical Driver Efficiency	94	%
Electrical Generator Efficiency	90	%

Table A4
GSC, Extra Firing & Heat Recovery Exchanger Modelling Assumptions.

GSC, Extra Firing Combustor & Heat Exchanger		
Equipment/Item	***Value***	***Units***
GSC Reactor Pressure Drop	4	%
Combustor Pressure Drop	20	kPa
Combustor Outlet Temperature	1360	ºC
Heat Recovery Exchanger Temperature Approach	10	ºC
Heat Recovery Exchanger Pressure Loss /side	10	kPa

Table A5
Power Plant Feedstock Characteristics.

Coal		**Natural Gas**	
Element	% weight	Component	% mole
C	66.52	C1	96.96
H	3.78	C2	1.37
O	5.46	C3	0.45
N	1.56	nC4	0.15
S	0.52	nC5	0.02
Moisture	8	C6 +	0.01
Ash	14.15	N2	0.86
		CO2	0.18
Properties		**Conditions**	
LHV (MJ/kg)	24.99	T (ºC)	25
HHV (MJ/kg)	25.80	P (bar)	20

Table A6
Power Island Modelling Assumptions.

Gas Turbine		
Equipment/Item	***Value***	***Units***
Air Compressor Polytropic Efficiency	90	%
Gas Turbine Isentropic Efficiency	92	%
Pressure Ratio	20	–
Air Filter Pressure Loss	1	%
Air Compressor Leakage	0.75	% inlet flow
Gas Turbine Auxiliary Consumption	0.35	% net power
Gas Turbine Mechanical Efficiency	99.86	%
Generator Efficiency	98.7	%
Steam Turbine		
Equipment/Item	***Value***	***Units***
Steam HP/IP/LP Stage Isentropic Efficiency	92/94/88	%
Condensing Pressure	0.048	bar
Turbine Mechanical Efficiency	99.6	%
Generator Efficiency	98.5	%
Water Pumps Adiabatic Efficiency	80	%
Power for Heat Rejection	0.008	MJe/MJth
Heat Recovery Steam Generators		
Equipment/Item	***Value***	***Units***
HP/IP/LP Pressure Levels	144/36/4	bar
Gas-Gas Temperature Minimum Approach	20	ºC
Pinch Point	10	ºC
Approach Point	5	ºC
Maximum SH/RH Steam Temperature	565	ºC
Minimum Stack Outlet Temperature	80	ºC
Economizer Pressure Loss	1	%
Evaporator Pressure Loss	4	%
Superheater Pressure Loss	3	%
HRSG Air Pressure Loss	3	kPa
HRSG Reduction Gases Pressure Loss	6	%
HRSG Heat Loss	0.7	% heat transferred

adding additional gaseous fuel combustion after the GSC reactors. When such an arrangement is implemented, the GSC-IGCC efficiency is increased by 3.7%-points when firing with syngas and 5.2%-points when firing with natural gas. Overcoming the second challenge by implementing a heat exchanger to transfer heat from the CO_2-stream (which goes only to the bottoming cycle) to the air stream (which goes through the full combined cycle) and redesigning the HRSGs increases the efficiency by a further 2%-points. Combined, these two strategies cancel out the 5.7%-point GSC-IGCC energy penalty.

Additional firing with carbon-containing gases decreases the CO_2 capture ratio and future work will therefore investigate the integration of efficient H_2 production processes with integrated CO_2 capture based on the gas switching reactor principle. H_2 produced in this way can then be used for additional firing without CO_2 emissions. However, the

Table A7
Simulations Cases Power Plant Summary.

Case	Base Case	A1	A2	B1	B2	C1	C2	C3	C4	D1	D2	D3	D4	E1	E2
TIT (°C)	1154,5	1153,5	1154,3	1169,4	1179,2	1360	1360	1360	1360	1360	1360	1360	1360	1360	1360
GSC Air Outlet Temperature (°C)	1154,5	1153,5	1154,3	1169,4	1179,2	1150,3	1150,4	1150,3	1150,4	1150,9	1150,6	1150,9	1150,6	1164,5	1164,5
Gas Turbine (MW)	200,9	199,7	207,3	221,0	233,4	227,7	231,3	289,3	294,3	259,8	266,1	344,3	354,9	280,8	365,1
Steam Turbine (MW)	228,8	219,3	210,2	216,7	204,2	229,9	223,2	279,3	267,1	215,4	201,0	261,4	240,4	199,1	245,8
Steam Pumps (MW)	2,473	2,3	2,5	2,5	2,4	2,3	2,5	3,0	3,2	2,8	2,8	3,2	3,3	2,5	3,0
Heat Rejection (MW)	3,1	3,0	2,9	2,9	2,8	3,0	2,8	3,6	3,4	2,6	2,6	3,4	3,2	2,6	3,2
Syngas Recycle Compressor (MW)	1,2	1,1	1,2	1,2	0,4	1,2	1,2	1,2	1,2	1,2	1,2	1,2	1,2	1,2	1,2
CO_2 Compression (MW)	12,9	12,7	12,7	12,9	12,9	9,8	9,8	12,8	12,7	9,5	9,5	12,8	12,8	9,8	12,9
ASU (MW)	38,7	38,7	38,7	38,7	38,7	38,7	38,7	38,7	38,7	38,7	38,7	38,7	38,7	38,7	38,7
Other Auxiliaries (MW)	5,6	4,5	5,2	4,3	4,3	5,3	5,3	5,8	5,8	5,4	5,4	6,0	6,1	4,5	5,1
Gross Power (MW)	429,7	419,1	417,3	437,7	437,6	457,6	454,5	568,6	561,4	475,2	467,1	605,7	595,3	479,9	610,9
Net Power (MW)	366,2	356,7	354,1	375,3	376,1	397,3	394,2	503,6	496,3	415,0	406,9	540,4	530,0	420,7	546,7
LHV Input (MW)	847,9	847,9	847,9	847,9	847,9	847,9	847,9	1041,0	1041,0	847,9	847,9	1076,0	1081,0	847,9	1074,0
Gross LHV Efficiency (%)	50,7	49,4	49,2	51,6	51,6	54,0	53,6	54,6	53,9	56,1	55,1	56,3	55,1	56,6	56,9
Net LHV Efficiency (%)	43,2	42,1	41,8	44,3	44,4	46,9	46,5	48,4	47,7	49,0	48,0	50,2	49,0	49,6	50,9
CO_2 Capture (%)	93,1	93,2	92,8	93,1	93,0	67,8	67,6	82,4	82,1	64,4	64,2	80,7	80,3	66,4	80,7
CO_2 Emissions (kg / MWh)	55,4	56,4	59,6	54,1	55,0	238,4	241,4	116,3	119,7	252,2	260,3	121,3	126,9	234,8	119,7

Table A8
Main Stream Summary for Case E2. Coal and Natural Gas Compositions are described in Table A5 in the Appendix A.

Property	Mass Flow (kg/s)	MW (kg/kmol)	P (bar)	T (°C)	Composition %mol									
Steam					N_2	O_2	Ar	CO	CO_2	CH_4	H_2	H_2O	H_2S	SO_2
1	33,9	15,5	1,0	25,0	South African Douglas Premium Coal									
2	167,1	23,5	44,0	900,0	1,06	0,00	1,41	61,22	8,55	0,10	20,85	6,63	0,18	0,00
3	100,4	23,5	42,1	300,0	1,06	0,00	1,41	61,22	8,55	0,10	20,85	6,63	0,18	0,00
4	69,3	23,5	42,2	888,0	1,06	0,00	1,41	61,22	8,55	0,10	20,85	6,63	0,18	0,00
5	69,3	23,5	20,1	889,1	1,06	0,00	1,41	61,22	8,55	0,10	20,85	6,63	0,18	0,00
6	107,3	36,5	19,3	1154,0	2,97	0,42	1,39	0,00	68,15	0,00	0,00	26,88	0,00	0,18
7	107,3	36,5	19,2	457,3	2,97	0,42	1,39	0,00	68,15	0,00	0,00	26,88	0,00	0,18
8	78,5	43,6	150,0	42,8	2,10	0,34	1,30	0,00	96,02	0,00	0,00	0,00	0,00	0,22
9	23,7	43,6	88,0	56,0	2,10	0,34	1,30	0,00	96,02	0,00	0,00	0,00	0,00	0,22
10	889,7	28,9	1,0	15,0	77,29	20,73	0,92	0,00	0,00	0,00	0,00	1,01	0,00	0,00
11	883,0	28,9	20,1	447,3	77,29	20,73	0,92	0,00	0,00	0,00	0,00	1,01	0,00	0,00
12	883,0	28,9	20,1	552,3	77,29	20,73	0,92	0,00	0,00	0,00	0,00	1,01	0,00	0,00
13	845,0	28,7	19,3	1164,0	80,03	17,4	0,96	0,00	0,20	0,00	0,00	1,12	0,00	0,00
14	849,6	28,6	19,1	1360,0	79,52	15,4	0,95	0,00	1,16	0,00	0,00	2,99	0,00	0,00
15	849,6	28,6	1,3	599,5	79,52	15,4	0,95	0,00	1,16	0,00	0,00	2,99	0,00	0,00
16	849,6	28,6	1,0	111,5	79,52	15,4	0,95	0,00	1,16	0,00	0,00	2,99	0,00	0,00
17	128,8	28,6	1,0	15,0	77,29	20,73	0,92	0,00	0,00	0,00	0,00	1,01	0,00	0,00
18	30,6	32,3	44,8	22,9	1,25	95,0	3,75	0,00	0,00	0,00	0,00	0,00	0,00	0,00
19	138,4	18,0	144,0	565,0	0,00	0,00	0,00	0,00	0,00	0,00	0,00	100,00	0,00	0,00
20	55,4	18,0	153,0	450,8	0,00	0,00	0,00	0,00	0,00	0,00	0,00	100,00	0,00	0,00
21	149,9	18,0	36,0	565,0	0,00	0,00	0,00	0,00	0,00	0,00	0,00	100,00	0,00	0,00
22	164,5	18,0	0,0	32,2	0,00	0,00	0,00	0,00	0,00	0,00	0,00	100,00	0,00	0,00
23	1,3	18,0	51,8	300,0	0,00	0,00	0,00	0,00	0,00	0,00	0,00	100,00	0,00	0,00
24	4,6	16.6	20,1	25,0	Natural Gas									

highly efficient partial capture GSC-IGCC plants (68–82% CO_2 capture) will still be appealing in an environment with low-to-moderate CO_2 prices. When CO_2 prices eventually become very high, these plants can be retrofitted for H_2-firing to maximize CO_2 avoidance.

To maximize the CO_2 capture or minimize the amount of extra H_2 required, it is important that the GSC reactor is operated at high temperatures. For example, it was found that reducing the maximum GSC temperature from 1200 to 1000 °C reduced CO_2 capture by 23.8%-points. Maximizing the reactor temperature introduces some technical challenges related to the oxygen carrier material as well as downstream switching valves and filters

The GSC-IGCC plant also offers two opportunities for exceeding the efficiency of an unabated benchmark plant. Firstly, the high steam partial pressure in the CO_2-rich stream from the GSC reduction stage allows for most of the condensation enthalpy to be recovered, resulting in an efficiency gain as much as 1%-point.

Secondly, pre-combustion gas clean-up can potentially be replaced with post-combustion gas clean-up because pollutants will remain concentrated in the CO_2-rich stream (when extra firing is done with clean natural gas or H_2). This strategy can achieve efficiency gains of 1.1% and 2.2%-points relative to hot and cold pre-combustion gas clean-up respectively. Literature studies have shown that certain oxygen carriers can tolerate the presence of sulphur compounds, suggesting that this is a viable strategy. It should be noted, however, that post-combustion gas clean-up with syngas extra firing will result in substantial SOx emissions, making natural gas the more attractive choice for extra firing in this case.

Finally, the best achievable efficiencies from GSC-IGCC configurations with additional syngas and natural gas firing were shown to be 49.6% and 50.9% respectively, significantly outperforming the unabated IGCC benchmark. GSC therefore has the potential to not only eliminate the energy penalty of CO_2 capture, but to even exceed the efficiency of plants without CO_2 capture. This is a potentially game-changing prospect for CCS and more detailed studies into the different

efficiency enhancement pathways identified in this work are therefore strongly recommended.

Process economics will be the subject of future work, but it can be mentioned here that the added capital costs of the additional combustor and recuperator will be minor and may be cancelled out by avoidance of pre-combustion gas clean-up. In comparison to previous economic assessments of CLC-IGCC plants (Cloete et al., 2018c; Mancuso et al., 2017), capital and fuel costs will be similar, but electricity output will be almost 20% more, leading to substantial reductions in the levelized cost of electricity. Future studies will quantify this economic advantage as well as the trade-offs related to reduced CO_2 capture ratios.

Appendix A

Acknowledgements

The authors gratefully acknowledge the financial support from the ERA-NET cofund, ACT GaSTech Project number 276,321 co-funded by the European Commission under the Horizon 2020 program, ACT Grant Agreement No. 691712. The partners collaborating in this article have received funding from MINECO, Spain (reference PCIN-2017-013) and the Research Council of Norway, Norway. The authors would also like to acknowledge Honeywell for the free Academic License of Unisim Design Suite R451, which enabled integrated GSC model & power plant simulations.

References

Abad, A., Adánez, J., Cuadrat, A., García-Labiano, F., Gayán, P., de Diego, L.F., 2011. Kinetics of redox reactions of ilmenite for chemical-looping combustion. Chem. Eng. Sci. 66, 689–702.
Abad, A., Adánez, J., Gayán, P., de Diego, L.F., García-Labiano, F., Sprachmann, G., 2015. Conceptual design of a 100 MWth CLC unit for solid fuel combustion. Appl. Energy 157, 462–474.
Altfeld, K., Schley, P., 2012. Klaus Altfeld, Peter Schley, Gas Quality.
BP, 2018. Statistical Review of World Energy. British Petroleum.
Campanari, S., Mastropasqua, L., Gazzani, M., Chiesa, P., Romano, M.C., 2016. Predicting the ultimate potential of natural gas SOFC power cycles with CO2 capture – part B: applications. J. Power Sources 325, 194–208.
Cloete, S., Romano, M.C., Chiesa, P., Lozza, G., Amini, S., 2015. Integration of a Gas Switching Combustion (GSC) system in integrated gasification combined cycles. Int. J. Greenh. Gas Control. 42, 340–356.
Cloete, S., Gallucci, F., van Sint Annaland, M., Amini, S., 2016. Gas switching as a practical alternative for scaleup of chemical looping combustion. Energy Technol. 4, 1286–1298.
Cloete, S., Zaabout, A., Romano, M.C., Chiesa, P., Lozza, G., Gallucci, F., van Sint Annaland, M., Amini, S., 2017. Optimization of a Gas Switching Combustion process through advanced heat management strategies. Appl. Energy 185 (Part 2), 1459–1470.
Cloete, S., Giuffrida, A., Romano, M., Chiesa, P., Pishahang, M., Larring, Y., 2018a. Integration of chemical looping oxygen production and chemical looping combustion in integrated gasification combined cycles. Fuel 220, 725–743.
Cloete, S., Tobiesen, A., Morud, J., Romano, M., Chiesa, P., Giuffrida, A., Larring, Y., 2018c. Economic assessment of chemical looping oxygen production and chemical looping combustion in integrated gasification combined cycles. Int. J. Greenh. Gas Control. 78, 354–363.
Dawson, B.K., Siegmund, S.C., Yonggui, Z., 2004. Flowsheet optimization for multi-product air separation units. The First Baosteel Annual Academic Conference.
de Diego, L.F., García-Labiano, F., Gayán, P., Abad, A., Cabello, A., Adánez, J., Sprachmann, G., 2014. Performance of Cu- and Fe-based oxygen carriers in a 500 Wth CLC unit for sour gas combustion with high H2S content. Int. J. Greenh. Gas Control. 28, 168–179.
Denton, D.L., 2014. An update on RTI's warm syngas cleanup demonstration project. Gasification Technologies Conference.
Gimeno, B., Artal, M., Velasco, I., Fernández, J., Blanco, S.T., 2018. Influence of SO2 on CO2 transport by pipeline for carbon capture and storage technology: evaluation of CO2/SO2 cocapture. Energy Fuels 32, 8641–8657.
Giuffrida, A., Romano, M.C., Lozza, G.G., 2010. Thermodynamic assessment of IGCC power plants with hot fuel gas desulfurization. Appl. Energy 87, 3374–3383.
Giuffrida, A., Romano, M.C., Lozza, G., 2013. Efficiency enhancement in IGCC power plants with air-blown gasification and hot gas clean-up. Energy 53, 221–229.
Hakonsen, S.F., Blom, R., 2011. Chemical looping combustion in a rotating bed reactor - finding optimal process conditions for prototype reactor. Environ. Sci. Technol. 45, 9619–9626.
Hamers, H.P., Gallucci, F., Cobden, P.D., Kimball, E., van Sint Annaland, M., 2013. A novel reactor configuration for packed bed chemical-looping combustion of syngas. Int. J. Greenh. Gas Control. 16, 1–12.
Han, L., Deng, G., Li, Z., Wang, Q., Ileleji, K.E., 2017. Integration optimisation of elevated pressure air separation unit with gas turbine in an IGCC power plant. Appl. Therm. Eng. 110, 1525–1532.
Heidenreich, S., 2013. Hot gas filtration – a review. Fuel 104, 83–94.
Higman, C., van der Burgt, M., 2008. Gasification 2nd Edition, Section 5.3.3.
Huang, J., Schmidt, K.G., Bian, Z., 2011. Removal and conversion of tar in syngas from woody biomass gasification for power utilization using catalytic hydrocracking. Energies 4, 1163.
IEA, 2018. Tracking Clean Energy Progress. International Energy Agency. http://www.iea.org/tcep/.
IPCC, 2014. Fifth Assessment Report: Mitigation of Climate Change. Intergovernmental Panel on Climate Change.
Ishida, M., Zheng, D., Akehata, T., 1987. Evaluation of a chemical-looping-combustion power-generation system by graphic exergy analysis. Energy 12, 147–154.
Jones, D., Bhattacharyya, D., Turton, R., Zitney, S.E., 2011. Optimal design and integration of an air separation unit (ASU) for an integrated gasification combined cycle (IGCC) power plant with CO2 capture. Fuel Process. Technol. 92, 1685–1695.
Kehlhofer, R., Hannemann, F., Rukes, B., Stirnimann, F., 2009. Combined-Cycle Gas & Steam Turbine Power Plants, Chapter 5, Figure 5-60. PennWell Books.
Kim, W.-S., Lee, J.-W., 2014. Improvement of the corrosion resistance by using enamel coating applied to the carbon steel fin tubes of the HRSG. J. Mech. Sci. Technol. 28, 2901–2908.
Kolster, C., Mechleri, E., Krevor, S., Mac Dowell, N., 2017. The role of CO2 purification and transport networks in carbon capture and storage cost reduction. Int. J. Greenh. Gas Control. 58, 127–141.
Kotowicz, J., Brzęczek, M., 2018. Analysis of increasing efficiency of modern combined cycle power plant: a case study. Energy 153, 90–99.
Kuusik, R., Trikkel, A., Lyngfelt, A., Mattisson, T., 2009. High temperature behavior of NiO-based oxygen carriers for Chemical Looping Combustion. Energy Procedia 1, 3885–3892.
Lyngfelt, A., 2014. Chemical-looping combustion of solid fuels – status of development. Appl. Energy 113, 1869–1873.
Lyngfelt, A., Leckner, B., 2015. A 1000 MWth boiler for chemical-looping combustion of solid fuels – discussion of design and costs. Appl. Energy 157, 475–487.
Lyngfelt, A., Leckner, B., Mattisson, T., 2001. A fluidized-bed combustion process with inherent CO2 separation; application of chemical-looping combustion. Chem. Eng. Sci. 56, 3101–3113.
Mancuso, L., Cloete, S., Chiesa, P., Amini, S., 2017. Economic assessment of packed bed chemical looping combustion and suitable benchmarks. Int. J. Greenh. Gas Control. 64, 223–233.
Marx, J., Schreiber, A., Zapp, P., Haines, M., Hake, J.F., Gale, J., 2011. Environmental evaluation of CCS using life cycle assessment–a synthesis report. Energy Procedia 4, 2448–2456.
Matthew, E.B.-H., Nick, F., Paul, S.F., 2016. Investigations into the effects of volatile biomass tar on the performance of Fe-based CLC oxygen carrier materials. Environ. Res. Lett. 11, 115001.
Mattisson, T., Keller, M., Linderholm, C., Moldenhauer, P., Rydén, M., Leion, H., Lyngfelt, A., 2018. Chemical-looping technologies using circulating fluidized bed systems: status of development. Fuel Process. Technol. 172, 1–12.
Noorman, S., van Sint Annaland, M., Kuipers, 2007. Packed bed reactor technology for chemical-looping combustion. Ind. Eng. Chem. Res. 46, 4212–4220.
Ohtsuka, Y., Tsubouchi, N., Kikuchi, T., Hashimoto, H., 2009. Recent progress in Japan on hot gas cleanup of hydrogen chloride, hydrogen sulfide and ammonia in coal-derived fuel gas. Powder Technol. 190, 340–347.
Robie, R.A., Hemingway, B.S., 1995. Thermodynamic Properties of Minerals and Related Substances at 298.15 K and 1 Bar (10^5 Pascals) Pressure and at Higher Temperatures, Bulletin, - Ed.
Rubin, E.S., Davison, J.E., Herzog, H.J., 2015. The cost of CO2 capture and storage. Int. J. Greenh. Gas Control. 40, 378–400.
Rydén, M., Arjmand, M., 2012. Continuous hydrogen production via the steam–iron reaction by chemical looping in a circulating fluidized-bed reactor. Int. J. Hydrogen Energy 37, 4843–4854.
Spallina, V., Romano, M.C., Chiesa, P., Gallucci, F., van Sint Annaland, M., Lozza, G., 2014. Integration of coal gasification and packed bed CLC for high efficiency and near-zero emission power generation. Int. J. Greenh. Gas Control. 27, 28–41.
Spallina, V., Pandolfo, D., Battistella, A., Romano, M.C., Van Sint Annaland, M., Gallucci, F., 2016. Techno-economic assessment of membrane assisted fluidized bed reactors for pure H2 production with CO2 capture. Energy Convers. Manage. 120, 257–273.
Srivastava, R.K., Jozewicz, W., Singer, C., 2001. SO2 scrubbing technologies: a review. Environ. Prog. 20, 219–228.
Stull, D.R., Prophet, H., 1971. JANAF Thermochemical Tables, 2nd edition ed. National Bureau of Standards U.S.
UNFCCC, 2015. Historic Paris Agreement on Climate Change, United Nations Framework Convention on Climate Change.

Wang, S., Wang, G., Jiang, F., Luo, M., Li, H., 2010. Chemical looping combustion of coke oven gas by using Fe2O3/CuO with MgAl2O4 as oxygen carrier. Energy Environ. Sci. 3, 1353–1360.
Wassie, S.A., Gallucci, F., Zaabout, A., Cloete, S., Amini, S., van Sint Annaland, M., 2017. Hydrogen production with integrated CO2 capture in a novel gas switching reforming reactor: proof-of-concept. Int. J. Hydrogen Energy 42, 14367–14379.
Zaabout, A., Cloete, S., Johansen, S.T., Annaland, Mv.S., Gallucci, F., Amini, S., 2013. Experimental demonstration of a novel gas switching combustion reactor for power production with integrated CO2 capture. Ind. Eng. Chem. Res. 52, 14241–14250.
Zaabout, A., Cloete, S., Annaland, Mv.S., Gallucci, F., Amini, S., 2015. A novel gas switching combustion reactor for power production with integrated CO2 capture: sensitivity to the fuel and oxygen carrier types. Int. J. Greenh. Gas Control. 39, 185–193.
Zaabout, A., Cloete, S., Amini, S., 2017. Autothermal operation of a pressurized Gas Switching Combustion with ilmenite ore. Int. J. Greenh. Gas Control. 63, 175–183.
Zaabout, A., Cloete, S., Tolchard, J.R., Amini, S., A pressurized gas switching combustion reactor: autothermal operation with a CaMnO3-δ-based oxygen carrier. Chemical Engineering Research and Design.
Zerobin, F., Pröll, T., 2017. Potential and limitations of power generation via chemical looping combustion of gaseous fuels. Int. J. Greenh. Gas Control. 64, 174–182.
Zhu, Q., 2015. High Temperature Syngas Coolers. IEA Clean Coal Center.